

Energy Principles of Scientific Breakeven in an Inertial Fusion Experiment

O. A. Hurricane¹,* D. A. Callahan¹,† D. T. Casey¹, A. R. Christopherson, A. L. Kritcher¹, O. L. Landen¹, S. A. Maclaren¹, R. Nora¹, P. K. Patel,[†] J. Ralph, D. Schlossberg¹, P. T. Springer, C. V. Young¹, and A. B. Zylstra¹
Lawrence Livermore National Laboratory, P.O. Box 808, L-472, Livermore, California 94550, USA

 (Received 27 October 2023; accepted 20 December 2023; published 5 February 2024)

Fusion “scientific breakeven” (i.e., unity target gain G_{target} , total fusion energy out > laser energy input) has been achieved for the first time (here, $G_{\text{target}} \sim 1.5$). This Letter reports on the physics principles of the design changes that led to the first controlled fusion experiment, using laser indirect drive, on the National Ignition Facility to produce target gain greater than unity and exceeded the previously obtained conditions needed for ignition by the Lawson criterion. Key elements of the success came from reducing “coast time” (the time duration between the end of the laser pulse and implosion peak compression) and maximizing the internal energy delivered to the “hot spot” (the yield producing part of the fusion fuel). The link between coast time and maximally efficient conversion of kinetic energy into internal energy is explained. The energetics consequences of asymmetry and hydrodynamic-induced mixing were part of high-yield big radius implosion design experimental and design strategy. Herein, it is shown how asymmetry and mixing consolidate into one key relationship. It is shown that mixing distills into a kinetic energy cost similar to the impact of implosion asymmetry, shifting the threshold for ignition to higher implosion kinetic energy—a factor not normally included in most statements of the generalized Lawson criterion, but the key needed modifications clearly emerge.

DOI: [10.1103/PhysRevLett.132.065103](https://doi.org/10.1103/PhysRevLett.132.065103)

Controlled thermonuclear fusion has been a dream of numerous scientists since the 1920s, when Eddington first suggested that the fusion of hydrogen into helium powers the Sun and stars. Hydrogen fusion has far too low a reaction rate for terrestrial uses. Thus, since the 1950s, fusion research has focused upon deuterium (D) and tritium (T) isotopes of hydrogen as the most accessible reaction for laboratory studies, in particular, the reaction $D + T \rightarrow n(14.1 \text{ MeV}) + {}^4_2\text{He}(3.5 \text{ MeV})$, where the energetic helium by-products, ${}^4_2\text{He}$, are also termed alpha particles. The α particles, which carry 20% of the fusion energy produced, can deposit their energy inside the fusion plasma region via Coulomb collisions with electrons, which in a collisional plasma rapidly thermalizes, thus raising the plasma thermal temperature (T_{th}). Since the D + T fusion reaction rate ($\langle\sigma v\rangle$) rapidly increases with T_{th} ($\langle\sigma v\rangle = 4.2 \times 10^{-20} T_{\text{th}}^{3.6} \text{ cm}^3/\text{s}$ in the $3.5 < T_{\text{th}} < 6.5 \text{ keV}$ range and $3.2 \times 10^{-19} T_{\text{th}}^{2.6} \text{ cm}^3/\text{s}$ in the $7 < T_{\text{th}} < 12 \text{ keV}$ range), self-heating can generate a nonlinear feedback process with rapid amplification of T_{th} and fusion yield production rate, $dY/dt = 5mQ_{\alpha}$, where $Q_{\alpha} = 8.2 \times 10^{24} \rho \langle\sigma v\rangle$, in $\text{GJ}/(\text{g} \cdot \text{s})$, is heating power per unit hot plasma

mass (m) from α particles produced by fusion, ρ is the hot plasma density, and t is time.

If the self-heating energy exceeds the externally applied energy needed to first make the D + T plasma hot, then a “burning plasma” state [1] is generated. If the self-heating power exceeds all the sources of cooling in the D + T plasma for sufficient time, then the burning plasma will “ignite,” generating a thermodynamic instability leading to a faster-than-exponential increase in T_{th} and Y . The plasma conditions needed to generate the thermodynamic instability of ignition are extremely difficult to obtain in the laboratory, but the requirements can be estimated using a variety of Lawson-like criteria [2]. The milestones of significant alpha-particle self-heating [3,4], burning plasmas [5–7], and ignition [2,8–10] have already been obtained using the laser indirect-drive (LID) inertially confined fusion (ICF) approach.

In LID ICF, a carefully designed laser pulse, carried by multiple laser beams, is incident upon the interior of metallic volume—a hohlraum—via small apertures termed laser-entrance holes (LEHs) which are at the two ends of the hohlraum with cylindrical geometry. As the laser energy is absorbed into the interior wall of the hohlraum, the laser energy is reradiated as a bath of x rays, characterized by a radiation temperature ($T_{\text{rad}} \sim 310 \text{ eV}$ at peak levels) that varies in time and space. The typical low gas-fill hohlraum energy accounting [11] is $\sim 50\%$ of the unscattered laser energy ends up in the hohlraum wall, $\sim 30\%$ – 35% of the laser energy is radiated back out the LEHs, $\sim 10\%$ – 15% is

Published by the American Physical Society under the terms of the [Creative Commons Attribution 4.0 International license](https://creativecommons.org/licenses/by/4.0/). Further distribution of this work must maintain attribution to the author(s) and the published article's title, journal citation, and DOI.

absorbed by the capsule (depends upon hohlraum to capsule surface area), and $\sim 5\%$ of the laser energy is absorbed into both the helium gas inside the hohlraum and the thin plastic membranes (“windows”) that seal the LEH. The T_{rad} , in turn, generates an ablation pressure p_{abl} around the surface of a spherical capsule suspended in the center of the hohlraum, within which resides DT fuel. The capsule is a hollow shell of material that is meant to absorb, in a thin layer called the ablation front, the hohlraum x rays and explode in response to the rapid ionization that occurs (the ablation process); the resulting $p_{\text{abl}} \sim 150$ Mbar drives the capsule inward upon itself—an implosion. The thin layer of DT fusion fuel, that was initially cryogenically “layered” onto the interior of the capsule [12], is accelerated inward during the implosion process, ultimately achieving velocities of several hundred km/s (~ 400 km/s in the case of the results of this and companion papers [13–15]) and considerable kinetic energy (~ 20 kJ) for its mass (~ 200 μg).

Combined with the ablator material remaining at the end of the implosion acceleration process (usually $\sim 5\%$ of the initial ablator mass and, coincidentally, typically close to the DT fuel mass), the DT fuel plus remaining ablator form a high-density shell that behaves as a piston doing pdV work on the central hot-spot volume V of the implosion, heating it. The per unit mass power balance in an ICF plasma that determines T_{th} is (see Refs. [16,17] for the form below)

$$c_{\text{DT}} \frac{dT_{\text{th}}}{dt} = f_{\alpha} Q_{\alpha} - f_B Q_{B,\text{DT}} - Q_e - \frac{1}{m} p \frac{dV}{dt}, \quad (1)$$

where $c_{\text{DT}} = 0.115$ GJ/(g · keV) is the DT plasma heat capacity [18], f_{α} is the fraction of the alpha-particle energy transferred by collisions to the hot spot, $Q_{B,\text{DT}} = 3.1 \times 10^7 \rho \sqrt{T_e}$ is the bremsstrahlung emission per unit mass for an equimolar DT mixture at electron temperature T_e , $Q_e = 5.9 \times 10^3 T_e^{7/2} / (\rho R^2)$ is the electron conduction loss (assuming a Spitzer [19] form but could also be the more modern SESAME [20] conductivity form which has a slightly weaker T_e and ρ dependence), and R is the time-dependent hot-spot radius [Q 's in units of in GJ/(g · s)]. The factor f_B , explored later in this Letter, is the fraction of x rays lost from the hot plasma, which is < 1 if the optical depth of the hot region is high enough to reabsorb x rays or > 1 if the presence of high- Z material enhances x-ray loss beyond that of pure DT. Since ICF hot spots are ultrahigh energy density and highly collisional, thermal equilibrium ($T_e \approx T_{\text{th}}$) is generally a good assumption.

With an expression for the rate at which hot-spot mass is generated by the ablation of DT fuel due to alpha deposition and electron heat conduction, $dm/dt = [m/(c_{\text{DT}} T_{\text{th}})] [(1 - f_{\alpha}) Q_{\alpha} + Q_e]$ [21], Eq. (1) can be time integrated from the time of peak implosion velocity to the time of peak hot-spot internal energy in order to find a relation for the total pdV done on the hot spot. Namely,

$$E_{pdV,\text{hs}} = E_{\text{hs}} - \frac{1}{5} Y_{1/2} + \int m f_B Q_B dt, \quad (2)$$

where $Y_{1/2} \approx Y_{\text{total}}/2$ is the fusion yield at the time of peak hot-spot internal energy. Since a fraction of the pdV work done by the shell of the implosion is expended on compressing the cold fuel and increasing its internal energy E_{fuel} , the total pdV work on all the DT is

$$E_{pdV} \approx E_{\text{hs}} + E_{\text{fuel}} - \frac{q}{10} Y_{\text{total}}, \quad (3)$$

where in the last expression the x-ray energy loss has been lumped into a “implosion quality” q , fitting factor on the total fusion yield Y_{total} . With Eq. (3), an expression for the fusion fuel energy gain, $G_{\text{fuel}} = Y_{\text{total}}/E_{pdV}$, can be found and compared to data (see Fig. 1). Namely,

$$G_{\text{fuel}} = \frac{Y_{\text{total}}}{E_{pdV}} = \frac{\frac{Y_{\text{total}}}{E_{\text{hs}}}}{1 + \frac{E_{\text{fuel}}}{E_{\text{hs}}} - \frac{q}{10} \frac{Y_{\text{total}}}{E_{\text{hs}}}}, \quad (4)$$

where

$$\frac{Y_{\text{total}}}{E_{\text{hs}}} = \frac{5 \int_0^{\tau} m Q_{\alpha} dt}{c_{\text{DT}} m T} \approx 4.6 \times 10^{26} p_{\text{hs}} \tau \frac{\langle \sigma v \rangle (T_{\text{hs}})}{T_{\text{hs}}^2}, \quad (5)$$

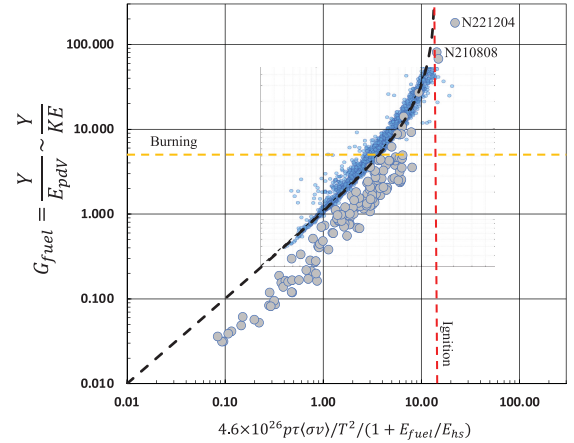


FIG. 1. A plot of G_{fuel} estimated from Y_{total}/KE from theory (solid black line), ensemble simulations database [25] using the HYDRA code [26] of N210808-like implosions (smaller blue dots), and NIF DT implosion experiments (larger gray dots). Error bars suppressed for clarity but are $\sim 25\%$ on the abscissa and $\sim 15\%$ on the ordinate. Fuel energy gain $G_{\text{fuel}} \sim 160$ resulted from NIF experiment N221204 [13–15] (exceeded by experiment N220729, not shown), with the next highest, $G_{\text{fuel}} \sim 70$ from N210808 already being in the ignition regime [2,8–10]. Unity G_{fuel} was achieved many years ago [3], when the first indications of alpha-heating feedback were observed. $G_{\text{fuel}} \sim 5$ corresponds to a burning plasma [5–7], where in the plot above the curve begins to notably curve upward. Thermonuclear instability, causing an explosive increase in T and, therefore, G_{fuel} is noted on the plot by the vertical dashed line.

where τ is the burn duration. The above relations show that G_{fuel} is directly related to a generalized Lawson [23] criterion-like parameter [24].

When compared to ensemble simulations [25] using the HYDRA code [26] (Fig. 1), it is seen that both the simulations and data from National Ignition Facility (NIF) DT implosion experiments are reasonably well fitted by Eqs. (4) and (5) with a choice of $q = 0.7$. The point at which G_{fuel} becomes very large is interpreted as an ignition condition and is very similar to the $E_\alpha/(2E_{\text{hs}}) > 1.4$ (half the alpha deposited energy over hot-spot energy) condition in Ref. [27]. Ultimately, G_{fuel} is limited by the amount of fusion fuel available to burn and the burn efficiency ϕ . The burn efficiency is limited by the disassembly (explosion) of the burning mass of DT fuel [28] which terminates the burn. The maximum G_{fuel} can be estimated from the total number of fusion reactions possible [$\phi m_{\text{fuel}}/(2\bar{A}m_p)$, $\bar{A} = 2.5$ being the average atomic mass of DT and m_p being the proton mass], the total yield per DT fusion (17.6 MeV) divided by the fuel kinetic energy ($m_{\text{fuel}}v_{\text{imp}}^2/2$), which gives $G_{\text{fuel,max}} \approx 7.52 \times 10^{-3} \phi (c/v_{\text{imp}})^2$, where c is the speed of light.

While G_{fuel} is directly related to fusion plasma conditions, the capsule gain G_{cap} , which measures the fusion yield to capsule energy absorbed ratio, and the target gain G_{target} , which measures the fusion yield to laser energy input into the hohlraum in an LID ICF target, are related to G_{fuel} through various energy efficiency factors [29]. Thus, for the same fusion plasma conditions, G_{fuel} is fixed, but G_{cap} and G_{target} will be design dependent and, therefore, only qualitative metrics of ignition. In fact, a modest to weak correlation between capsule or target absorbed energy and fusion yield is exhibited in NIF LID DT implosion data [30]. Table I shows all three gain metrics for a variety of NIF DT implosions. The milestone of $G_{\text{fuel}} > 1$ was achieved in 2013 [3], $G_{\text{cap}} > 1$ was achieved in 2021 [2,8–10], and $G_{\text{target}} > 1$, also termed “scientific break-even,” was achieved in December 2022 and is the result reported here and in companion papers [13–15,31].

As can be observed from Eqs. (4) and (5), as well as Fig. 1, G_{fuel} is determined by $p\tau$, T_{th} , and the ratio of fuel to hot-spot internal energy ($E_{\text{fuel}}/E_{\text{hs}}$). In order to maximize gain, it is clear that the $p\tau$ and T_{th} should be maximized (at least until the temperature-dependent reaction rate peaks)—a well-known fact in fusion.

Since ICF implosions are very well modeled by classical mechanics and thermodynamics, determining what properties of the implosion design should be altered in order to maximize $p_{\text{hs}}\tau$ and T_{hs} can be understood with the following relations based upon a piston-model abstraction of an implosion [34,35]. Namely, for a pdV work-dominated implosion, by equating Q_e in Eq. (1) with pdV specific power, one obtains $T_{\text{hs}}^{7/2} \sim p_{\text{hs}}v_{\text{imp}}R_{\text{hs}}$ and from the piston model [35] $v_{\text{imp}}R_{\text{hs}} = \sqrt{4\pi c_1/[C(\alpha_{\text{if}})m_{\text{shell}}(1-f^2)]}$ with

TABLE I. Various gain metrics for select NIF experiments across four campaigns. Naming convention is “NYMMDD,” where N = NIF, YY = year, MM = month, and DD = day. For example, for N221204 the capsule absorbed energy is $Y_{\text{total}}/G_{\text{cap}} = 258$ kJ and the total energy deposited into the DT fuel is $Y_{\text{total}}/G_{\text{fuel}} = 19.4$ kJ of which $\sim 66\%$ goes into the hot spot. The 2 orders of magnitude expenditure of energy going from the laser to the DT fuel is typical of indirect-drive ICF schemes.

Shot	G_{fuel}	G_{cap}	G_{target}	Reference
N221204	160	12	1.5	This and [13–15]
N210808	70	5.8	0.72	[2,8–10]
N210207	7.8	0.75	0.09	[5–7]
N180128	4.5	0.34	0.031	[32]
N170601	4.3	0.32	0.03	[4]
N140120	2.2	0.17	0.014	[33]
N130927	1.3	0.09	0.008	[3]

$2\pi p_{\text{hs}}R_{\text{hs}}^3 = C(\alpha_{\text{if}})m_{\text{shell}}v_{\text{imp}}^2(1-f^2)/2$ all combining to give an expression for T_{hs} :

$$T_{\text{hs}} \sim \left[\frac{C(\alpha_{\text{if}})}{4\pi} m_{\text{shell}}(1-f^2) \right]^{4/7} \frac{v_{\text{imp}}^{10/7}}{c_1^{2/7}}, \quad (6)$$

where $C(\alpha_{\text{if}}) \sim 0.66$ is a dimensionless measure of the fraction of implosion kinetic energy directed into the hot spot (a number that can somewhat vary with in-flight adiabat α_{if}), $c_1 = p_{\text{pv}}R_{\text{pv}}^5$ is a measure of the hot-spot entropy of the implosion at peak velocity (pv), m_{shell} is the *stagnated* [24] shell mass (the DT fuel plus remaining ablator, at the time of minimum radius radially inward of the outgoing stagnation shock), and $f^2 = n\text{RKE}$ is the normalized residual kinetic energy [36] that is the fraction of kinetic energy unconverted into internal energy at the time of stagnation, the asymmetry component of which is determined by the hot-spot area weighted harmonic mean of shell areal density, $f^2 = 1 - \langle(\rho R)^{-1}\rangle^{-1}/\langle\rho R\rangle$, where $\langle \dots \rangle$ denotes the area average [35].

The main sources of asymmetry for low gas-fill hohlraum-driven implosions have been determined to be [37] peak laser power imbalances, diagnostic windows in the hohlraum, manufacturing gaps on the waist of the hohlraum, sag of the capsule suspended in the hohlraum by a formvar membrane called the “tent,” and manufacturing variation in the thickness of the capsule [38]. For experiment N221204, the roll-up of asymmetry impact, as determined by postexperiment simulations [14], is $f^2 \sim 0.07$.

The piston-model-derived Lawson parameter [23] scaling is

$$p_{\text{hs}}\tau \sim \frac{C^2(\alpha_{\text{if}})}{(4\pi)^2 c_1} m_{\text{shell}}^2 v_{\text{imp}}^3 (1-f^2)^2, \quad (7)$$

which scales with the product of shell momentum and kinetic energy. Thus, the key parameter [Eq. (5)] for increasing G_{fuel} scales as

$$p_{\text{hs}} \tau \frac{\langle \sigma v \rangle}{T_{\text{hs}}^2} \sim \frac{v_{\text{imp}}^{3+(10/7)(a-2)}}{c_1^{1+(2/7)(a-2)}} \left[\frac{C(\alpha_{\text{if}})}{4\pi} m_{\text{shell}} (1-f^2) \right]^{2+(4/7)(a-2)}, \quad (8)$$

where a is from a power-law approximation to the fusion reaction rate $\langle \sigma v \rangle \sim T_{\text{hs}}^a$ in the regime of interest ($2 < a < 4$ typically).

Qualitatively similar conclusions are obtained by examining alternative ignition metrics, $p_{\text{hs}}^2 E_{\text{hs}}$, $p_{\text{hs}} R_{\text{hs}}$, or $\rho R_{\text{hs}} T_{\text{hs}}$, that are all algebraically equivalent to each other, since it has been shown that in the regime of limited alpha heating $p_{\text{hs}}^2 E_{\text{hs}} = 2\pi(p_{\text{hs}} R_{\text{hs}})^3 \sim [m_{\text{shell}} c_s^2 (1-f^2)/R_{\text{pv}}^2]^3$ [34,35], where c_s is the hot-spot sound speed. With significant alpha heating, the parameter sensitivity in Eq. (8) changes to exponential and transcendental [39].

Equations (6)–(8) express the importance of increased m_{shell} , higher implosion velocities (together reflecting kinetic energy $\text{KE} = m_{\text{shell}} v_{\text{imp}}^2/2$ and momentum $m_{\text{shell}} v_{\text{imp}}$), minimal radius of peak velocity R_{pv} , and minimal asymmetry ($f^2 \sim 0$) in optimizing an ICF implosion for high G_{fuel} . R_{pv} is controlled by reducing an LID implosion’s “coast time” (the time duration between the end of the laser pulse and implosion peak compression) [41] by making this time a small fraction of the hohlraum cooling time [35]. This helps to maximize the implosion deceleration rate and rate of conversion of implosion kinetic energy into internal energy, which is key for achieving high stagnation pressures and stagnation temperatures.

Unfortunately, with a fixed hohlraum geometry, increasing capsule size by either radius or thickness and reducing coast time (which lengthens the duration of the laser pulse) make implosion symmetry control significantly more difficult [42]. In principle, symmetry is manageable if one considers trade-offs between parameters of the integrated hohlraum-capsule system [11] that defines an LID target and does considerable detailed design work [6,14]. While originally explained in terms of capsule scale rather than mass, the above paragraphs describe the high-yield big radius implosion design (HYBRID) strategy [16,17,43] for obtaining a burning plasma and ignition.

From the time-dependent hot-spot heat balance [Eq. (1)], the tipping point where the total alpha power balances the bremsstrahlung emission power defines the critical ignition temperature [44] T_{ign} . In the case of an ICF implosion, some radiation can be reradiated from the hot-spot edge (if the optical depth is sufficiently high) while some radiation escapes; thus, T_{ign} for an ICF implosion is determined by $Q_\alpha = f_B Q_B$, where $f_B = f_{\text{rerad}} \bar{Z}^2$ is a multiplier of the DT bremsstrahlung power per unit hot-spot mass that is a net measure of x-ray limitation coming from reradiation

($f_{\text{rerad}} \leq 1$; potentially as low as $f_{\text{rerad}} \sim 0.5$ for some designs) and enhancement due to mixing into the hot spot ($\bar{Z} > 1$ being the average atomic number of the DT plus whatever material has mixed into the DT). Clearly, enhanced x-ray losses from mixing and reradiation can offset each other. Thus, in the presence of uniform high- Z mixing into the hot DT, T_{ign} is modified [40] to $T_{\text{ign}} \approx 4.3 f_{\text{rerad}}^{0.3} \bar{Z}^{2.0.3}$ keV. Since the internal energy of DT is $E = c_{\text{DT}} m T_{\text{th}}$, it is expected that the KE required to reach thermodynamic instability threshold (i.e., “ignition”) increases with mixing relative to an identical ICF implosion with no mixing, by the scaling $\bar{Z}^{2.0.3}$. Namely,

$$\text{KE}_{\text{ign,mix}} \approx \text{KE}_{\text{ign,no-mix}} \bar{Z}^{2.0.3}, \quad (9)$$

where, like asymmetry, hot-spot mixing appears as an energy “cost” [45]. For mix to pollute the hot spot, it must penetrate radially inward through the surrounding cold fuel, implying some increase in the \bar{Z} of the cold fuel, but this effect is neglected in the relationships of this Letter. Equation (9) suggests that, in the relations of this Letter, the degradation due to asymmetry, quantified by $1-f^2$, can be replaced with $1/[(\langle \rho R \rangle)^{-1} \langle \rho R \rangle \bar{Z}^{2.0.3}]$ to account for both the degradation from asymmetry and hot-spot mixing. Comparing Eq. (9) to numerical models confirms the energy scaling (see Fig. 2). Seeds for mixing are largely from capsule defects [46,47] and/or the capsule fill tube [48], resulting in values of \bar{Z}^2 that can be variable experiment to experiment but are usually inferred to be in the range ~ 1 – 1.5 —a comprehensive analysis will be forthcoming [49], but a preliminary value of $\bar{Z}^2 \sim 1$ is inferred for N221204. For an example high mix case of $\bar{Z}^2 \sim 1.5$, the energy needed to reach the ignition threshold would move $1.13\times$ higher according to Eq. (9).

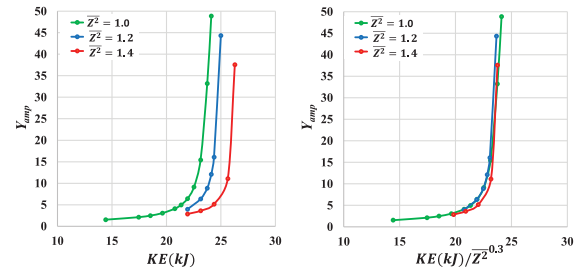


FIG. 2. Left: calculated yield amplification Y_{amp} from a numerical model [50] applied to experiment N210808 is plotted against implosion peak kinetic energy for the cases of no mixing into the hot spot ($\bar{Z}^2 = 1$), moderate mixing ($\bar{Z}^2 = 1.2$), and higher levels of mixing ($\bar{Z}^2 = 1.4$). The threshold for significant yield amplification moves to higher levels of KE with increased mixing (\bar{Z}). Right: The offset in KE with increased mixing appears to correspond to the expectation based upon Eq. (9), since the calculated curves overlay if the KE is scaled by $\bar{Z}^{2.0.3}$.

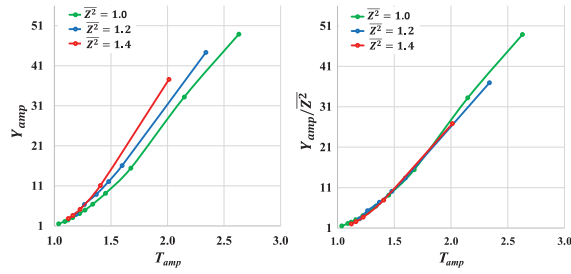


FIG. 3. Left: calculated yield amplification Y_{amp} from a numerical model based upon experiment N210808 is plotted against thermal temperature amplification for the cases of no mixing into the hot spot ($\bar{Z}^2 = 1$), moderate mixing ($\bar{Z}^2 = 1.2$), and higher levels of mixing ($\bar{Z}^2 = 1.4$). With more mix, a higher level of yield amplification is required to achieve a fixed level of thermal temperature amplification T_{amp} , thus making ignition harder to achieve. Right: The curves overlay if Y_{amp} is scaled by \bar{Z}^2 .

Since there is an energy cost to mixing, it is expected that the Lawson criterion for ignition should also be altered in the presence of hot-spot mixing, which is common in ICF experiments. The criterion of Ref. [40] [also see Eq. (1) in companion Letter [13]] reflects the energy cost of mixing by shifting the ignition boundary to higher T_{th} , which is why this criterion is generally plotted as multiple curves in a two-dimensional space of $p\tau$ vs T_{th} [2,13,15], effectively blurring the location of the ignition boundary (a reflection of the three-dimensional parameter space, $p\tau$, T_{th} , and \bar{Z} ; see Fig. 4). Other formulations of the Lawson criterion generally have not included the possibility of mix-induced bremsstrahlung altering the hot-spot energy balance, but, like Eq. (9), a correction to these criteria can be found via the mathematical connection between the measure of fusion yield amplification due to α heating, Y_{amp} , and a given Lawson-like criterion by noting that

$$Y_{\text{amp,no-mix}} \approx Y_{\text{amp,mix}}/\bar{Z}^2, \quad (10)$$

which is confirmed by comparing to numerical models (see Fig. 3) that show a higher Y_{amp} is required to achieve a fixed level of temperature amplification (T_{amp}) in the presence of hot-spot mixing. Thus, most ICF Lawson-like criteria can or should be modified to include mixing as shown in Table II, the result being a more stringent condition for ignition (see Fig. 4).

Thus, hot-spot mixing has two primary effects, cooling the hot-spot plasma for a fixed amount of implosion KE and moving the tipping point of ignition to a higher and harder to achieve threshold, thus requiring more KE to compensate for both effects. The energy “cost” of mixing is compounded with asymmetry, which also reduces the effective implosion KE that can be used to increase the internal energy of an ICF hotpot. The implosion performance degrading impacts of mix and asymmetry, if not

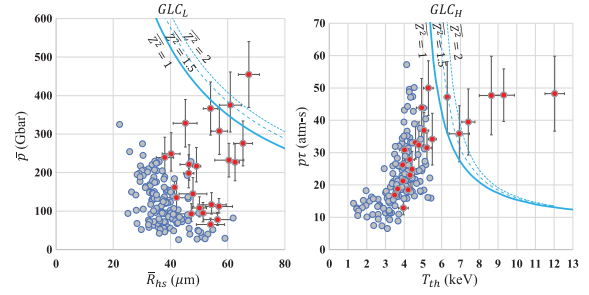


FIG. 4. Various published Lawson-like criteria for ICF ignition are plotted with the Table II correction for mixing included. Left: The $GLC_L = (\bar{p}/420 \text{ Gbar})(\bar{R}_{\text{hs}}/50 \mu\text{m}) \geq 1$ criterion [51] (solid curve) becomes $(\bar{p}/420 \text{ Gbar})(\bar{R}_{\text{hs}}/50 \mu\text{m}) \geq 1 + 0.24 \ln(\bar{Z}^2)$ (dashed and dotted curves). In this criterion, \bar{p} and \bar{R}_{hs} are the burn and time-average hot-spot pressure and radius, respectively. Right: The criterion of Ref. [40], which originally included the effect of mixing in the theory, is also shown in the companion Letter [13]. A key feature to note in the right frame is the greatly increased burn-averaged T_{th} at nearly fixed burn-averaged $p\tau$, as the series of experiments passes the ignition criterion. Gray points are all NIF DT implosion data, while red points are from the Hybrid-E series of experiments.

perfectly controlled, can both be offset with additional implosion kinetic energy to “pay” for the wasted energy. Additionally, one-dimensional implosion performance also increases with KE. Increasing KE through increased v_{imp} risks additional ablation Rayleigh-Taylor instability, despite applying high-foot [3,53–55] mitigation tactics as has been done in NIF ICF DT implosion experiments since 2014. The cooling of the hot-spot plasma can create a secondary effect of higher implosion convergence (as measured by shell areal density $\rho_{\text{shell}}\delta R$), which can be beneficial for increased fusion yield (since fusion burn efficiency increases with $\rho_{\text{shell}}\delta R$) if the implosion is robust enough to ignite and propagate despite the additional KE cost of mixing—this situation is presently not typical in ICF.

Increasing KE with increased m_{shell} is the alternative to velocity, but controlling the asymmetry of bigger capsules makes asymmetry control in hohlraums much more difficult due to the longer time duration of the laser pulse

TABLE II. Select published Lawson-like criterion “corrected” to account for hot-spot mixing. Here, mixing moves the metrics threshold for ignition to a higher value. Here, “criterion” > “ignition threshold” implies ignition.

Criterion	Ignition threshold	Reference
ITFX $_{\alpha}$	$(3.39 + 1.11 \ln \bar{Z}^2)^2$	[52]
χ_{α}	$(2.71 + \ln \bar{Z}^2)^{0.83}$	[1]
GLC $_L$	$1.0 + 0.24 \ln \bar{Z}^2$	[2,51]
F_{α}	$(1.52 + 0.59 \ln \bar{Z}^2)^{0.8}$	[27]

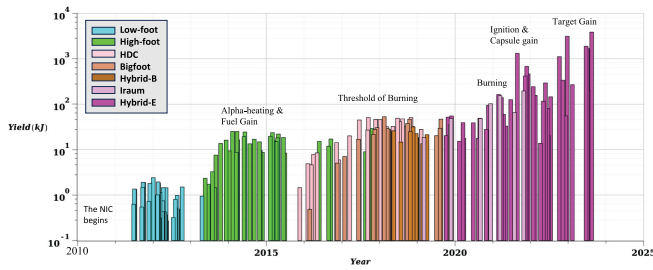


FIG. 5. A subset of fusion yields from DT implosion experiments on the NIF that illustrate the dates of key steps. The different implosion designs listed in the key are explained in detail in Refs. [2,13], and references therein.

needed for thicker shells (shock transit time) and reduced hohlraum to capsule radius ratio (“case-to-capsule” ratio) which reduces the smoothing of the x-ray intensity at the capsule ablation front. However, an improved understanding of hohlraum symmetry control in low gas-fill hohlraums [42,56] and the demonstration of the effectiveness of cross-beam energy transfer (originally demonstrated in high gas-fill hohlraums [57]) in low gas-fill hohlraums as a tool to move laser energy between beams for symmetry control [58,59] both indicated that symmetry with larger-scale capsules may be manageable. Thus, increasing KE with increased capsule scale (m_{shell}) was the strategy [16,17,43] followed, initially with larger radius capsules (a choice that maintains v_{imp} with fixed laser energy and hohlraum efficiency) and then later with thicker capsules (accessible as hohlraum efficiency and NIF laser energy improved) [60]. In an implosion, additional KE is most useful if the time duration over which the KE is converted into hot-spot internal energy is short with minimal coasting. By designing an implosion to have coast time shorter than the hohlraum cooling time, R_{pv} is minimized, which maximizes T_{hs} , p , and ρR [35,41,61]. However, the laser pulse durations associated with short coast times are long, which, like capsule thickness, makes symmetry control more difficult; thus, each series of DT experiments usually started with longer coast times until good symmetry was obtained and then worked toward shorter coast times in incremental predictor-corrector-like steps to reacquire symmetry control as the laser pulse length increased.

While experimentally intensive, this strategy has been successful, yielding more than an $\sim 2800\times$ increase in G_{fuel} (Fig. 1) and more than an $\sim 6000\times$ factor in fusion yield (Fig. 5) over a decade of work with the attainment of a ICF burning plasma [5–7], igniting plasma [2,8–10], and, most recently, target gain [13–15], also known as scientific breakeven.

O. A. H. thanks emeritus LLNL Director William “Bill” Goldstein and former LLNL ICF Program Director M. John Edwards for their support of the HYBRID strategy. This work was performed under the auspices of U.S.

Department of Energy by Lawrence Livermore National Laboratory under Contract No. DE-AC52-07NA27344. This document was prepared as an account of work sponsored by an agency of the U.S. Government. Neither the U.S. Government nor Lawrence Livermore National Security, LLC, nor any of their employees makes any warranty, expressed or implied, or assumes any legal liability or responsibility for the accuracy, completeness, or usefulness of any information, apparatus, product, or process disclosed, or represents that its use would not infringe privately owned rights. Reference herein to any specific commercial product, process, or service by trade name, trademark, manufacturer, or otherwise does not necessarily constitute or imply its endorsement, recommendation, or favoring by the U.S. Government or Lawrence Livermore National Security, LLC. The views and opinions of authors expressed herein do not necessarily state or reflect those of the U.S. Government or Lawrence Livermore National Security, LLC, and shall not be used for advertising or product endorsement purposes.

*hurricane1@llnl.gov

†Present address: Focused Energy Inc., 11525-B Stonehollow Drive, Suite 200, Austin, Texas 78758, USA.

- [1] R. Betti, A. R. Christopherson, B. K. Spears, R. Nora, A. Bose, J. Howard, K. M. Woo, M. J. Edwards, and J. Sanz, *Phys. Rev. Lett.* **114**, 255003 (2015).
- [2] H. Abu-Shawareb *et al.* (Indirect Drive ICF Collaboration), *Phys. Rev. Lett.* **129**, 075001 (2022).
- [3] O. A. Hurricane *et al.*, *Nature (London)* **506**, 343 (2014).
- [4] S. Le Pape, L. F. Berzak Hopkins, L. Divol *et al.*, *Phys. Rev. Lett.* **120**, 245003 (2018).
- [5] A. Zylstra, O. Hurricane *et al.*, *Nature (London)* **601**, 542 (2022).
- [6] A. Kritcher, C. Young, H. Robey *et al.*, *Nat. Phys.* **18**, 251 (2022).
- [7] J. S. Ross *et al.*, [arXiv:2111.04640](https://arxiv.org/abs/2111.04640).
- [8] A. L. Kritcher, A. B. Zylstra, D. A. Callahan, O. A. Hurricane *et al.*, *Phys. Rev. E* **106**, 025201 (2022).
- [9] A. B. Zylstra, A. L. Kritcher, O. A. Hurricane, D. A. Callahan *et al.*, *Phys. Rev. E* **106**, 025202 (2022).
- [10] O. A. Hurricane, *Proceedings of the 2022 IEEE International Conference on Plasma Science (ICOPS)* (IEEE, New York, 2022).
- [11] D. A. Callahan *et al.*, *Phys. Plasmas* **27**, 072704 (2020).
- [12] B. J. Koziolowski, E. R. Mapoles, J. D. Sater, A. A. Chernov, J. D. Moody, J. B. Lugten, and M. A. Johnson, *Fusion Sci. Technol.* **59**, 14 (2011).
- [13] H. Abu-Shawareb *et al.* (Indirect Drive ICF Collaboration), preceding Letter, *Phys. Rev. Lett.* **132**, 065102 (2024).
- [14] A. L. Kritcher, A. Zylstra, C. Weber, O. A. Hurricane *et al.*, companion paper, *Phys. Rev. E* **109**, 025204 (2024).
- [15] A. Pak, A. B. Zylstra *et al.*, companion paper, *Phys. Rev. E* **109**, 025203 (2024).
- [16] O. A. Hurricane *et al.*, *Plasma Phys. Controlled Fusion* **61**, 014033 (2019).
- [17] O. A. Hurricane *et al.*, *Phys. Plasmas* **26**, 052704 (2019).

- [18] Note that in ICF, and fusion, in general, the fusion plasma is not in thermal equilibrium with the radiation field, since the photon mean-free path is very long compared to the size of the plasma, so the blackbody energy density ($4\sigma T^4/c$ with σ being the Stefan-Boltzmann constant and c being the speed of light) is not included in the heat capacity.
- [19] L. Spitzer and R. Härm, *Phys. Rev.* **89**, 977 (1953).
- [20] S. P. Lyon and J. D. Johnson, Sesame: The Los Alamos National Laboratory equation of state database, Technical Report No. LA-UR-92-3407, Los Alamos National Laboratory, 1995.
- [21] There are legitimate theoretical concerns that this dm/dt expression underestimates the mass ablation rate [22], but the present expression appears to be sufficient for capturing the data trends described in this Letter.
- [22] W. Daughton, B. J. Albright, S. M. Finnegan, B. M. Haines, J. L. Kline, J. P. Sauppe, and J. M. Smidt, *Phys. Plasmas* **30**, 012704 (2023).
- [23] J. D. Lawson, *Proc. Phys. Soc. London Sect. B* **70**, 6 (1957).
- [24] R. Betti *et al.*, *Phys. Plasmas* **17**, 058102 (2010).
- [25] R. C. Nora, N. Birge, D. Casey *et al.*, *Phys. Plasmas* **30**, 092705 (2023).
- [26] M. M. Marinak, G. D. Kerbel, N. A. Gentile, O. Jones, D. Munro, S. Pollaine, T. R. Dittrich, and S. W. Haan, *Phys. Plasmas* **8**, 2275 (2001).
- [27] A. R. Christopherson, R. Betti, S. Miller, V. Gopalaswamy, O. M. Mannion, and D. Cao, *Phys. Plasmas* **27**, 052708 (2020).
- [28] G. S. Fraley, E. J. Linnebur, R. J. Mason, and R. L. Morse, *Phys. Fluids* **17**, 474 (1974).
- [29] M. D. Rosen, *Phys. Plasmas* **6**, 1690 (1999).
- [30] A. Zylstra, O. Hurricane, D. Callahan, A. Kritcher, O. Landen, J. Lindl, A. Pak, P. Patel, J. Ralph, J. Ross, and C. Young, *Nucl. Fusion* **61**, 116066 (2021).
- [31] M. S. Rubery *et al.*, following Letter, *Phys. Rev. Lett.* **132**, 065104 (2024).
- [32] K. L. Baker, C. A. Thomas, D. T. Casey *et al.*, *Phys. Rev. E* **102**, 023210 (2020).
- [33] T. Döppner, D. A. Callahan, O. A. Hurricane *et al.*, *Phys. Rev. Lett.* **115**, 055001 (2015).
- [34] O. A. Hurricane *et al.*, *Phys. Plasmas* **27**, 062704 (2020).
- [35] O. A. Hurricane *et al.*, *Phys. Plasmas* **29**, 012703 (2022).
- [36] A. L. Kritcher, R. Town, D. Bradley, D. Clark, B. Spears, O. Jones, S. Haan, P. T. Springer, J. Lindl, R. H. H. Scott, D. Callahan, M. J. Edwards, and O. L. Landen, *Phys. Plasmas* **21**, 042708 (2014).
- [37] B. J. MacGowan, O. L. Landen, D. T. Casey *et al.*, *High Energy Density Phys.* **40**, 100944 (2021).
- [38] D. T. Casey *et al.*, *Phys. Rev. Lett.* **126**, 025002 (2021).
- [39] For example, p in $pV^\gamma = p_{pv} V_{pv}^\gamma \exp[p\tau H(T)]$, where $H(T)$ is a complicated function of T , describes the jump in pV^γ after stagnation in the presence of significant α heating [40].
- [40] O. A. Hurricane, S. A. Maclaren, M. D. Rosen, J. H. Hammer, P. T. Springer, and R. Betti, *Phys. Plasmas* **28**, 022704 (2021).
- [41] O. A. Hurricane *et al.*, *Phys. Plasmas* **24**, 092706 (2017).
- [42] D. A. Callahan *et al.*, *Phys. Plasmas* **25**, 056305 (2018).
- [43] O. A. Hurricane, D. A. Callahan, M. J. Edwards *et al.*, in *Proceedings of the 59th Annual Meeting of the American Physical Society Division of Plasma Physics (Vol. 62, No. 12, abstract PO7.00001)*, Milwaukee, WI, 2017 (unpublished).
- [44] R. F. Post, *Rev. Mod. Phys.* **28**, 338 (1956).
- [45] Relation (9) suggests a way to assess the energy cost of “wetted foam” fuel configurations of interest to inertial fusion energy applications. However, Eq. (9) clearly does not include the impact of cold mix into the DT fuel layer, which can stiffen the compression properties of the fuel layer, creating an additional energy cost beyond Eq. (9). We speculate, but do not prove, that the compressional energy cost should scale with pressure, $\sim(\bar{Z} + 1)/\bar{A}$, where \bar{A} is the average atomic mass of the mixture.
- [46] A. B. Zylstra, D. T. Casey, A. Kritcher *et al.*, *Phys. Plasmas* **27**, 092709 (2020).
- [47] T. Braun, S. Kucheyev, S. Shin, Y. Wang, J. Ye, N. T. Jr, C. Saw, D. Bober, E. Sedillo, N. Rice, K. Sequoia, H. Huang, W. Requieron, A. Nikroo, D. Ho, S. Haan, A. Hamza, C. Wild, and J. Biener, *Nucl. Fusion* **63**, 016022 (2022).
- [48] A. Pak *et al.*, *Phys. Rev. Lett.* **124**, 145001 (2020).
- [49] L. Divol *et al.* (private communication).
- [50] O. A. Hurricane *et al.*, *Nat. Phys.* **12**, 800 (2016).
- [51] J. D. Lindl, S. W. Haan, O. L. Landen, A. R. Christopherson, and R. Betti, *Phys. Plasmas* **25**, 122704 (2018).
- [52] P. K. Patel *et al.*, *Phys. Plasmas* **27**, 050901 (2020).
- [53] D. E. Hinkel *et al.*, *Plasma Phys. Controlled Fusion* **55**, 124015 (2013).
- [54] T. R. Dittrich *et al.*, *Phys. Rev. Lett.* **112**, 055002 (2014).
- [55] H.-S. Park *et al.*, *Phys. Rev. Lett.* **112**, 055001 (2014).
- [56] J. E. Ralph, O. Landen, L. Divol *et al.*, *Phys. Plasmas* **25**, 082701 (2018).
- [57] P. Michel, L. Divol, E. A. Williams *et al.*, *Phys. Rev. Lett.* **102**, 025004 (2009).
- [58] A. L. Kritcher *et al.*, *Phys. Rev. E* **98**, 053206 (2018).
- [59] L. A. Pickworth *et al.*, *Phys. Plasmas* **27**, 102702 (2020).
- [60] Since for LID x rays drive the implosion, $KE \sim \int \sigma T_{\text{rad}}^4 A_{\text{cap}} dt$, where A_{cap} is the capsule surface area and the time integration is over the period of the x-ray drive. Thus, $v_{\text{imp}} \sim T_{\text{rad,max}}^2 \sqrt{t_{\text{pulse}}/(\rho_{\text{shell}} \delta R)}$, where $T_{\text{rad,max}}$ is the maximum T_{rad} , t_{pulse} is the duration of the T_{rad} pulse, and $\rho_{\text{shell}} \delta R$ is the shell areal density. So, with increased shell thickness a higher T_{rad} is needed to maintain v_{imp} , which can be accomplished only with an improvement in hohlraum energy efficiency and/or increased laser energy delivery.
- [61] O. A. Hurricane, *J. Phys. Conf. Ser.* **717**, 012005 (2016).